# Atomistic simulations of low energy ion irradiation of 2D materials: From *ab-initio* molecular dynamics to simple binary collision model

Silvan Kretschmer and Arkady V. Krasheninnikov
*Institute of Ion Beam Physics and Materials Research, Helmholtz-Zentrum Dresden-Rossendorf, 01328 Dresden, Germany*

(Received 21 August 2024; accepted 7 November 2024; published 20 November 2024)

Ion irradiation is a powerful tool to tune the properties of two-dimensional (2D) materials by creating defects and introducing impurities. At the same time, efficient defect production and especially ion implantation into 2D materials require a careful choice of ion energies, as when energies are too low or too high, production of defects and implantation rate will be unsatisfactorily low. As for the bulk systems, various approaches have been employed to predict optimum ion energies for specific tasks, but they cannot always be directly applied to 2D materials. Here, we carry out *ab initio* molecular dynamics (MD) and analytical potential (AP) MD simulations and compare the results to those obtained with a simple binary collision approximation (BCA) model. We show that when chemical interactions between the ions and target atoms are essential, as in the case of B and N ion implantation into graphene, as compared to inert gas ions, the AP MD and the BCA model are inadequate. We further suggest a modified-BCA approach with the corrected displacement threshold energies, which account for chemical interactions between the ion and target atoms. The threshold energy can be obtained from first-principles calculations, and the modified-BCA model gives qualitatively and, for some ions, even quantitatively correct results for the energies corresponding to the onset of defect production and substitution probabilities, while being at the same time many orders of magnitude computationally less expensive than the first-principles MD. We show that in any case the BCA and modified-BCA calculations provide the upper and lower bounds on the optimum ion energy.

DOI: 10.1103/PhysRevMaterials.8.114003

## I. INTRODUCTION

Ion irradiation is one of the most powerful techniques to tune the properties of materials by creating defects in a controllable manner or introducing impurities [1,2]. Irradiation has also been shown to be an efficient tool for tailoring the characteristics of two-dimensional (2D) materials and making electronic devices (see Refs. [3–8] for an overview). In particular, ion implantation is a promising route to fabricate single-photon emitters [9–11], memristors [12], ultra-fast photo detectors [13], and controllable resistive random access memory [14] in 2D materials, as well as adding magnetic properties [15–17], increasing sensitivity for defect-mediated magnetic field detection [18], or creating catalytically active centers [4].

Impurities can be introduced into 2D materials directly by ion implantation [19–26] or, in principle, foreign atoms can fill vacancies created by energetic particles [27,28]. The first approach can be easier to implement provided that ion beam energy is properly chosen and the required (normally low) energy is achievable. While in bulk systems variations in ion energy give rise to small changes in the average implantation depth, it is intuitively clear that, due to their reduced dimensionality, direct implantation into truly 2D systems is possible only in a very narrow range of energies. If ion energy is too low, the ion will not be implanted and most likely desorb from the surface; if it is too high, the ion will go through the target and/or create too much additional damage. Thus, choosing the optimum ion energy corresponding to the highest probability for the ion to "get stuck" in the target is of paramount importance [24]. It is also clear that the optimum ion energy must be relatively low—a few tens or at most hundreds of eVs—normally much lower than what is used in ion implantation into bulk materials. The choice of ion energy is also crucial if atoms of specific types in multi-component 2D materials, e.g., $MoS_2$, are expected to be predominantly sputtered [29].

Atomistic computer simulations, including binary collision approximation (BCA) models [30,31] and more sophisticated analytical potential (AP) molecular dynamics simulations [32], can be employed to predict the optimum ion energy. Both approaches work rather well for bulk systems where the ion performs many collisions with the atoms of the target before it stops, but their applicability to 2D materials is questionable [33,34]. The problem is that neither of the methods properly describes chemical interactions between the atoms, while they are particularly important at low ion energies [35]. Besides, the transport of ions in matter (TRIM) [30] and similar codes treat the solid target as an amorphous structure with the same density—obviously not a good approximation when essentially one collision of the ion with the target atoms is expected.

The *ab initio* Born-Oppenheimer MD describes interatomic forces much more accurately than other atomistic approaches. Unfortunately, it is computationally very expensive for ion impact modeling, as many trajectories must be simulated. In this study, we compare all three approaches—*ab initio*, AP MD, and a simple BCA model—to obtain insights into the interplay of chemical interactions and the collective motion of the target atoms in the vicinity of the impact

 ©2024 American Physical Society

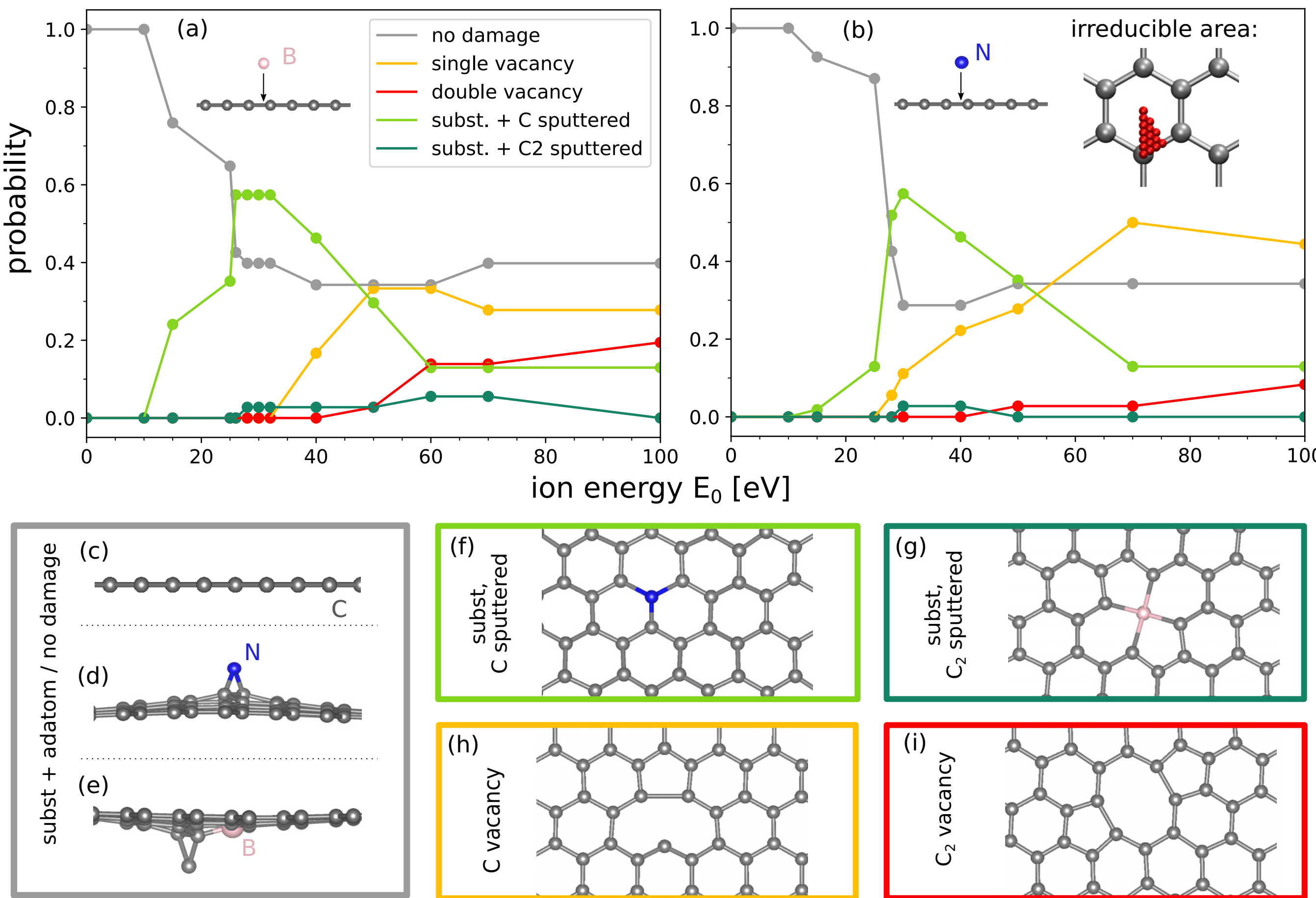


FIG. 1. Outcomes of B and N ion impacts onto free-standing graphene and illustration of the formed defect structures. Probabilities for different outcomes with or without defect formation for B (a) and N (b) ion impacts. The points are results of calculations (averaged over all impact points); curves are just guides to the eye. The insets schematically illustrate the simulation setup and visualize the impact points selected inside the irreducible area. [(c)-(i)] Side and top views of typical atomic configurations which appear after ion impacts.

location. By example of ion irradiation of single-layer graphene, we show that AP MD provides reasonable results for inert gas atoms, but overestimates optimum ion energies for B and N implantation into graphene due to the incorrect description of the energetics of the complex atomic configurations, which are far away from the standard 'training configuration set' used for the parametrization of the potential. We also suggest a modified-BCA approach which, with minimum input from the first-principles calculations (the ion displacement energy, that is the minimum ion energy required to produce a defect in graphene or in principle any other 2D material), can be used to very quickly access the optimum ion energy for the implantation into a 2D system.

## II. METHODS

*Ab initio* MD simulations were performed within the framework of density-functional theory (DFT), as implemented in the VASP package [36,37]. The Perdew-Burke-Ernzerhof (PBE) parametrization of the exchange and correlation functional [38] was used. The target system represented a rectangular graphene supercell consisting of 96 carbon atoms. Prior to carrying out the MD simulations, the system was carefully relaxed, with the criterion that the remnant forces are below 0.001 eV/Å. The plane-wave energy cutoff was chosen to be 400 eV and sampling over the Brillouin zone was performed using a $3 \times 3 \times 1$ k-point mesh. The MD simulations were carried out with the same parameters as structure optimization. In the MD runs, the projectile was initially placed 5 Å above the graphene layer with the velocity vector pointing toward the target system. The velocity was assigned according to the initial kinetic energy. The simulations were run with a time step of 0.1 fs. The simulations were performed for 16 different impact points in the irreducible area [see inset in Fig. 1(b)].

Although in what follows we use the word "ion" for the projectile, in the simulations it was a neutral atom. This approximation is physically meaningful, as singly charged ions with low energies (we consider ion energies below 100 eV) are expected to be neutralized before they interact with the surface [1]. We also note that the Born-Oppenheimer DFT MD cannot describe charge transfer in any case, while Ehrenfest dynamics combined with time-dependent DFT and classical approximation for the nuclei capable of accounting for charge transfer and electronic stopping [39–42] is computationally way too expensive for the simulations of defect production.

Analytical potential (AP) MD simulations were carried out with the LAMMPS code [43] using the B-C-N Tersoff

potential with a smoothly joint ZBL potential [44,45] at small distances for the description of graphene and its interaction with B, N ions [46]. Similar to the *ab initio* calculations, the input structure with 4032 C atoms was relaxed using this potential. Impact simulations were performed for the same time step and impact points relative to the atom positions as in the *ab initio* simulations.

As a relatively small amount of ion energy was deposited on average into vibrational degrees of freedom of the target, the typical temperature of the system after ion impact was of the order of 700 K and, as graphene network is very robust, the account for energy dissipation at the borders of the supercell in DFT MD simulations was not necessary. In the AP MD simulations, the thermostat regions at the boundaries were used, but obviously (for a much larger system than the one used in DFT MD) that had little effect on the results.

## III. RESULTS AND DISCUSSION

To assess the probability of B and N atoms to take substitutional positions upon low-energy ion irradiation, that is to be implanted into free-standing single layer graphene, we carried out DFT MD simulations, as described above. Figs. 1(a) and 1(b) show the probabilities for different outcomes of ion impacts as functions of ion energy, and corresponding atomic configurations are presented in Figs. 1(c)–1(i). These include, in addition to the impurities in substitutional positions shown in Fig. 1(f), single and double vacancies, in Figs. 1(h) and 1(i), and impurities in double vacancies, as in Fig. 1(g). Ions can also go through graphene without creating any damage [Fig. 1(c)], be adsorbed on graphene surface [Fig. 1(d)], or displace a C atom, but not sputter it [Fig. 1(e)]. As adatoms will likely desorb from graphene, and because our simulations indicate that the configuration seen in Fig. 1(e) can easily be converted to impurity adatom configuration (C adatom and substitutional B atom swap their positions), which is energetically much more favorable, we assumed that no damage was created in graphene and united the probabilities for the formation of these configurations.

The explanation of this general trend is intuitively clear: if the projectile has too low energy, it is either reflected or the adatoms are formed; if ion energy is too high, the projectile will go through or cause target atom sputtering, but cannot bind to the target system and leaves a vacancy behind. Only in a narrow energy window, the ion has enough energy to sputter one of the target atoms and replace it, with the ion energy after the collision being smaller than its binding energy to defective graphene. Hence, the consecutive appearance of adatom, substitutional, and vacancy configurations along the ion energy axis is the typical behavior upon low energy ion irradiation of 2D materials. For B and N implantation, it manifests itself in the high probabilities of adatom formation at energies below 20 eV, and the peaks observed in Fig. 1 at 30 eV (substitutional configurations) and 50 eV (vacancies). The lowest energies at which defects appear correspond to the (nearly) head-on collisions [35].

It is evident from the curves that the probabilities to create substitutional impurities in graphene have maxima at 29 eV and 30 eV for B and N ions, respectively, with the values reaching 62% and 60% for each. The presence of the peak on the curve "probability vs energy" is a general feature of low energy ion implantation into 2D materials, similar to defect production in 2D systems, as discussed earlier [8]. At higher energies the cross section for displacing a recoil atom decreases [5], and the ion goes through the atomically thin target, creating less and less damage.

Having calculated the probabilities for different atomic configurations to appear upon ion impacts using DFT MD, we carried out similar calculations by employing AP MD. The DFT and AP probabilities for B and N impurities substituting for single C atom are presented in Fig. 2, along with the corresponding atomic configurations in the insets. Although the number of impact points is much smaller than in the previous calculations [47]—we deliberately used the same number of points as in the DFT MD simulations—the results are in good agreement with the previously published data; the maxima on the curves are at about 60 eV, and the maximal probability is at about 40% for B and 55% for N. Although the qualitative behavior of the curves obtained using DFT MD is the same, the lowest energies at which ions are implanted and the maxima are at noticeably lower energies than those obtained in the AP MD simulations. This is related to the unsatisfactory description of the energetics of the complicated configurations when host C atoms are being replaced by B or N atoms. We also note that, according to the DFT calculations, a substantial number of impurities can be created at energies of about 20 eV, which is in agreement with the experimental results [19], where N impurities in graphene were observed after 25 eV ion implantation.

As evident from the comparison of the DFT and AP results, the latter cannot be used to reliably predict the implantation probabilities and defect production under low-energy ion irradiation. At the same time, as DFT MD simulations require much computational effort, it is desirable to have a more efficient method that would allow one quick estimates of the optimum energy and the probability to create substitutional impurities. In the following, we will derive a binary collision-based model modified for direct implantation into 2D materials.

In the binary collision approximation (BCA) the complex many-body interaction of the impinging projectile with the target atoms is reduced to a sequence of binary collisions, each singling out the major contribution, namely the interaction with the closest target atom. In this way, considering only binary collisions, the energy transfer can be calculated analytically or numerically. Moreover, for isolated single graphene sheet, only one binary collision takes place, which substantially simplifies the calculations.

To get information about the outcome of the ion impact into the 2D target, one should evaluate the scattering integral for given ion species, impact parameter $b$ and initial ion kinetic energy $E_0$. For screened potentials, such as the ZBL potential, the integral can be evaluated only numerically. The scattering angle $\theta_c$ in the center-of-mass frame can be calculated [1] from:

$$\theta_c = \pi - 2b \int_{r_0}^{\infty} \frac{\mathrm{d}r}{r^2} \frac{1}{\sqrt{1 - \frac{V(r)}{E_c} - \left(\frac{b}{r}\right)^2}}, \tag{1}$$

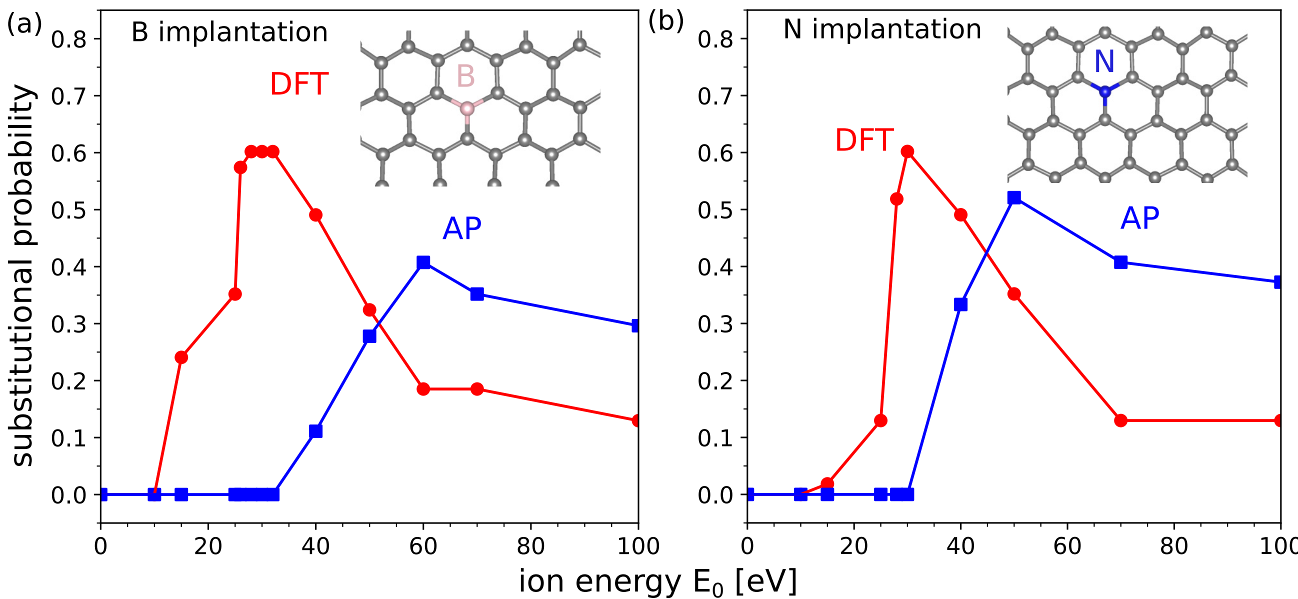


FIG. 2. Low-energy ion implantation. Implantation probability of ions into graphene as obtained from DFT and analytical potential (AP) MD simulations for B (a) and N (b) ions. Points are the results of calculations, lines are just guides to the eye. The insets show the atomic configurations of substitutional impurities in graphene.

where $b$ denotes the impact parameter, $V(r)$ is the interaction potential (here ZBL), $E_c = \frac{\mu}{m_1}E_0$ is the kinetic energy in the center-of-mass frame (with $m_1$ being the ion mass, and $\mu$ the reduced mass with $\mu^{-1} = m_1^{-1} + m_2^{-1}$). The distance of the closest encounter $r_0$ can be obtained as the root of the denominator. The transferred energy is then given by

$$T = T_{\max} \sin^2\left(\frac{\theta_c}{2}\right), \tag{2}$$

where $T_{\max}$ is the maximal transferable energy (in the head-on collision),

$$T_{\max} = \frac{4m_1m_2}{(m_1+m_2)^2}E_0 \tag{3}$$

for the binary collision of a nonrelativistic projectile (mass $m_1$, kinetic energy $E_0$) with the initially resting target atom (mass $m_2$).

In order to assess the accuracy of this simple approach, we computed sputtering yield for B, N, Ne, and Ar ions impinging onto graphene as functions of ion energies. The results for the *ab initio* MD (red), analytical potential MD (blue), and BCA model (green) calculations are shown in Fig. 3. Again, we find that the AP MD simulations yield systemically right-shifted sputtering probability distributions for B and N ions due to the overbinding of the AP. Within the BCA model, sputtering is accounted for by comparing the transferred energy from Eq. (2) to the displacement threshold energy $T_d$. The displacement threshold energy quantifies the minimum initial kinetic energy a target atom needs to leave the system. Electron beam experiments can be employed to estimate the displacement threshold energy, e.g., for graphene $T_d = 21.2$ eV is measured [48]. The latter value for $T_d$ is used in the BCA model. Whenever the transferred energy exceeds the displacement threshold

$$\text{sputtering condition: } T > T_d, \tag{4}$$

the target atom is sputtered.

The BCA sputtering yield for noble gas ions is in a remarkably good agreement with the *ab initio* results [Figs. 3(c) and 3(d)]. A slight shift of the BCA onset to lower ion energies can be understood by the neglect of the energy transferred to the atoms surrounding the primary target recoil atom (which is well described in the MD simulations). However, inert gas and target atoms do not chemically interact (only repulsive interaction at small separations), which explains why the BCA calculations with the displacement threshold energy taken from electron beam experiments give such a good fit.

The situation for B and N ions, with the results presented in Figs. 3(a) and 3(b), is different. There, the BCA results corresponding to displacement threshold, without account for chemical interactions between ion and target atom, underestimate the sputtering yield for ion energies below 70 eV, while showing reasonable agreement for higher energies. The onset of sputtering of these species, chemically similar to the target atoms, is better described by the reduced displacement threshold $T_d^r = T_d(C)_N = 10.2$ eV obtained from the head-on collision calculations [35], which account for ion-target bonding (orange line). $T_d^r$ can be derived from the energy transfer in a binary collision

$$T_d^r = \frac{4m_1m_2}{(m_1+m_2)^2}E_{\text{th}}^{\text{ion}}, \tag{5}$$

where $E_{\text{th}}^{\text{ion}}$ is the threshold *ion* energy (the minimum ion energy to sputter a target atom), which was calculated previously using DFT MD for graphene and h-BN [35]. Obviously, it is different for different impinging ions (chemical elements).

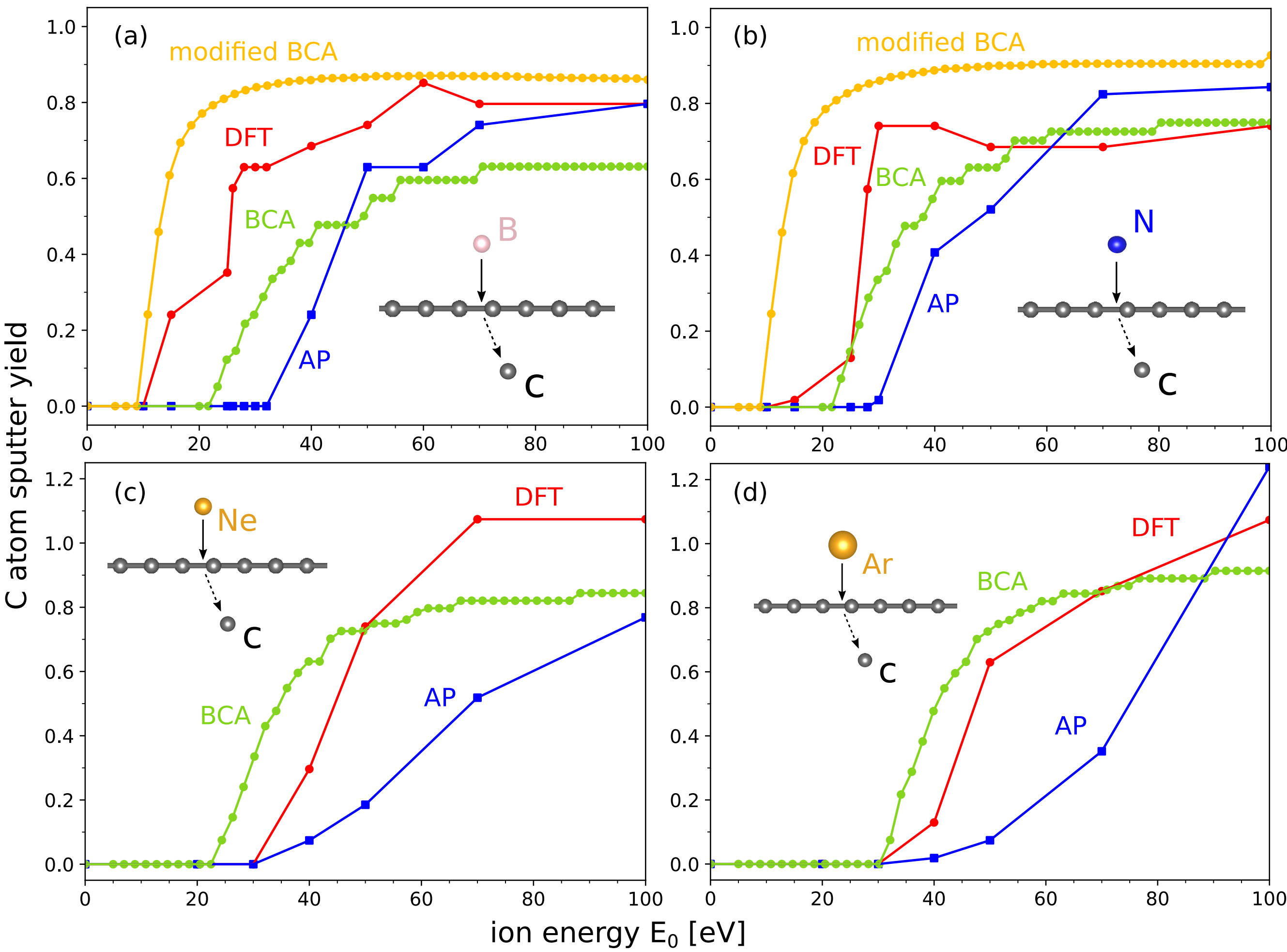


FIG. 3. Carbon atom sputtering yield under low-energy ion irradiation of graphene calculated using *ab initio* MD (red), analytical potential (AP) MD (blue), and a BCA scheme for B (a), N (b), Ne (c), and Ar (d) ions. In the BCA scheme, the displacement threshold for the C atom was chosen to be $T_d(C) = 21.2$ eV, as obtained by electron beam experiments (green). For B and N impacts, the BCA model accounting for chemical interactions (orange) between ion and target atoms is parametrized by the lowered displacement thresholds $T_d(C)_B = 9.1$ eV and $T_d(C)_N = 10.2$ eV.

Including the effect of chemical interactions between ion and target into the BCA model yields remarkable agreement with respect to the *ab initio* reference for low ion energy, but overestimates the sputtering yield for larger ion energies. Apparently, the chemical interaction between projectile and primary target atom is crucial for ion energies close to the displacement threshold. Its importance decreases with increasing ion energy. The effect of the ions chemical interaction vanishes at intermediate ion energies, where the sputtering yield approaches its maximum. From that point on, the BCA with the displacement threshold from electron beam experiments, which neglects chemical interactions, proves to be a better approximation for the binding environment.

Having introduced a modified-BCA model for the assessment of the sputtering yield, we also tried to apply it to the estimates of the probability of substitutional impurity formation. Modeling direct implantation requires a second condition to be fulfilled: The ion needs to be chemically bound to the target after it transferred part of its kinetic energy to a target atom, causing the recoil sputtering. Therefore, we require that its remaining kinetic energy $E_{\mathrm{fin}}$ after the collision is smaller than the typical binding energy $E_b$ of the atom to the system:

$$E_{\mathrm{fin}} = E_0 - T < E_b. \tag{6}$$

We stress that $E_b$ is not cohesive energy, but the energy needed to remove one atom from the system. For graphene, it is about 19 eV. Due to the chemical similarity of B, C, and N atoms—and in order to keep the number of parameters as small as possible—we assumed that the typical binding energy is given by the displacement threshold $E_b \approx T_d$ (and $T_d^r$, respectively) and carried out the modified-BCA calculations.

Figure 4 presents the resulting substitutional probabilities evaluated over the full irreducible area. Once more, the *ab initio* data acts as a reference. The AP results, which display a shift to higher energies, are shown for comparison. The substitutional probability calculated with the BCA model, based on the lowered displacement threshold due to chemical interactions between projectile and target atom, is in a good agreement with the *ab initio* MD results (though the optimum energy is slightly underestimated), a technique which is several orders of magnitude more computationally

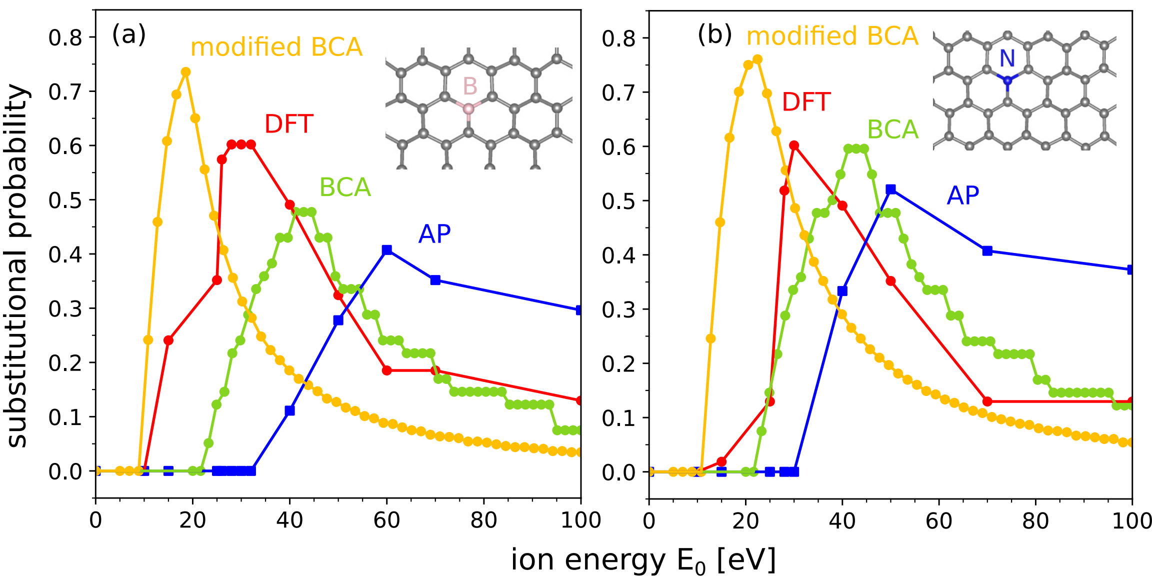


FIG. 4. Probabilities for direct ion implantation into graphene as functions of ion energies. Substitutional probabilities for B (a) and N (b) ions calculated based on *ab initio* MD, analytical potential MD, and the BCA scheme, respectively. Also the results of the modified-BCA model are presented, where the ion displacement energy is taken from the DFT calculations. The *ab initio* MD results serve as a benchmark addressing all effects relevant at low ion energies, namely, direct momentum transfer in binary collision with the closest target atom, chemical bonding of the target atom, and collective motion of the atoms in its vicinity.

expensive than the BCA model. For ion energies higher than the energy at which the maximum probability is reached, this model underestimates the probability. Conversely, the BCA model without chemical interactions gives good agreement at high energies (even a lot better than the AP results) and poor agreement at low energies (overestimation of the direct substitution onset). Hence, for ion energies lower than the maximum in substitutional probability, chemical interactions are important, while for higher ion energies the displacement threshold without chemical interactions is appropriate. Based on the above, it appears that the best strategy to find the energy optimal for the implantation is to run the BCA and modified-BCA calculations, which would give the upper and lower bounds on the value and take the averaged value as the best guess.

We note, however, that for the free-standing systems suspended over a trench in the substrate or deposited on a TEM grid, the probabilities given by the simulations can be higher than the experimental values. The reason for this is the self-annealing of defects and/or presence of dirt, e.g., amorphous carbon on the surface of the target 2D material. On the other hand, for 2D materials on a substrate [24,49], the diffusion of the implanted species between the substrate and the 2D material, and filling the vacancies can increase the substitution rate. The same processes can also strongly affect the concentration of defects in free-standing and supported 2D materials after irradiation, and the role of substrate can be different, depending on ion types and energies [50,51].

## IV. CONCLUSION

To conclude, we carried out atomistic simulations at the DFT, AP, and BCA levels of theory to get insights into the interaction of low-energy ions with graphene and assess the optimum energies for B and N ion implantation into graphene. We compared AP MD and BCA data to the results obtained using the computational much more expensive *ab initio* MD, and highlighted the differences. Specifically, the AP MD gives much higher optimum energies due to the incorrect account of chemical bonding. We note that machine-learning potentials [52,53] may improve the accuracy, but the computational cost of the parametrization for ion irradiation simulations is expected to be extremely high, as many far-from-equilibrium configurations should be accounted for. At the same time, we demonstrated that a modified-BCA model, which incorporates sputtering and bonding of the ion with the target atoms can reasonably well describe the situation with only one parameter: the reduced displacement threshold energy, which accounts for chemical interaction between the impinging ion and the target atoms, and for 2D materials can be obtained in a single DFT MD run, corresponding to the head-on collision [35] of the ion and a target atom.

The modified-BCA approach, which can be applied for various 2D materials and ions, gives qualitatively and even quantitatively correct results for the energies corresponding to the onset of defect production and substitution probabilities, while being at the same time many orders of magnitude computationally less expensive than the first-principles MD simulations. In general, the BCA and modified-BCA calculations can give the upper and lower bounds on the optimum ion energy.

## ACKNOWLEDGMENTS

We acknowledge funding from the German Research Foundation (DFG), projects KR 4866/9-1, and the

collaborative research center "Chemistry of Synthetic 2D Materials" CRC-1415-417590517. Generous CPU time grants from the Technical University of Dresden computing cluster (TAURUS) and Gauss Centre for Supercomputing e.V. [54], Supercomputer HAWK at Höchstleistungsrechenzentrum Stuttgart (HLRS) [55] are greatly appreciated.

[1] M. Nastasi, J. Mayer, and J. Hirvonen, *Ion-Solid Interactions - Fundamentals and Applications* (Cambridge University Press, Cambridge, 1996).
[2] K. Höflich, G. Hobler, F. I. Allen, T. Wirtz, G. Rius, L. McElwee-White, A. V. Krasheninnikov, M. Schmidt, I. Utke, N. Klingner, M. Osenberg, R. Córdoba, F. Djurabekova, I. Manke, P. Moll, M. Manoccio, J. M. De Teresa, L. Bischoff, J. Michler, O. De Castro *et al.*, Roadmap for focused ion beam technologies, Appl. Phys. Rev. **10**, 1041311 (2023).
[3] Z. Li and F. Chen, Ion beam modification of two-dimensional materials: Characterization, properties, and applications, Appl. Phys. Rev. **4**, 011103 (2017).
[4] M. Schleberger and J. Kotakoski, 2D material science: Defect engineering by particle irradiation, Materials **11**, 1885 (2018).
[5] A. V. Krasheninnikov and K. Nordlund, Ion and electron irradiation-induced effects in nanostructured materials, J. Appl. Phys. **107**, 071301 (2010).
[6] G.-Y. Zhao, H. Deng, N. Tyree, M. Guy, A. Lisfi, Q. Peng, J.-A. Yan, C. Wang, and Y. Lan, Recent progress on irradiation-induced defect engineering of two-dimensional $2H-MoS_2$ few layers, Appl. Sci. **9**, 678 (2019).
[7] M. Telkhozhayeva and O. Girshevitz, Roadmap toward controlled ion beam-induced defects in 2d materials, Adv. Funct. Mater. **34**, 2404615 (2024).
[8] A. V. Krasheninnikov, Are two-dimensional materials radiation tolerant? Nanoscale Horizons **5**, 1447 (2020).
[9] N. Mendelson, D. Chugh, J. R. Reimers, T. S. Cheng, A. Gottscholl, H. Long, C. J. Mellor, A. Zettl, V. Dyakonov, P. H. Beton, S. V. Novikov, C. Jagadish, H. H. Tan, M. J. Ford, M. Toth, C. Bradac, and I. Aharonovich, Identifying carbon as the source of visible single-photon emission from hexagonal boron nitride, Nat. Mater. **20**, 321 (2021).
[10] J. Klein, M. Lorke, M. Florian, F. Sigger, L. Sigl, S. Rey, J. Wierzbowski, J. Cerne, K. Müller, E. Mitterreiter, P. Zimmermann, T. Taniguchi, K. Watanabe, U. Wurstbauer, M. Kaniber, M. Knap, R. Schmidt, J. J. Finley, and A. W. Holleitner, Site-selectively generated photon emitters in monolayer $MoS_2$ via local helium ion irradiation, Nat. Commun. **10**, 2755 (2019).
[11] M. Fischer, J. M. Caridad, A. Sajid, S. Ghaderzadeh, M. Ghorbani-Asl, L. Gammelgaard, P. Bøggild, K. S. Thygesen, A. V. Krasheninnikov, S. Xiao, M. Wubs, and N. Stenger, Controlled generation of luminescent centers in hexagonal boron nitride by irradiation engineering, Sci. Adv. **7**, eabe7138 (2021).
[12] S. Aldana, J. Jadwiszczak, and H. Zhang, On the switching mechanism and optimisation of ion irradiation enabled 2D $MoS_2$ memristors, Nanoscale **15**, 6408 (2023).
[13] R. Chen, Y. Pei, Y. Kang, J. Liu, Y. Xia, J. Wang, H. Xu, C. Jiang, W. Li, and X. Xiao, A high-speed photodetector fabricated with tungsten-doped $MoS_2$ by ion implantation, Adv. Electron. Mater. **8**, 2200281 (2022).
[14] C. Yin, C. Gong, S. Tian, Y. Cui, X. Wang, Y. Wang, Z. Hu, J. Huang, C. Wu, B. Chen, X. Wang, and C. Li, Low-energy oxygen plasma injection of 2D $Bi_2Se_3$ realizes highly controllable resistive random access memory, Adv. Funct. Mater. **32**, 2108455 (2022).
[15] P. C. Lin, R. Villarreal, S. Achilli, H. Bana, M. N. Nair, A. Tejeda, K. Verguts, S. De Gendt, M. Auge, H. Hofsäss, S. De Feyter, G. Di Santo, L. Petaccia, S. Brems, G. Fratesi, and L. M. Pereira, Doping graphene with substitutional Mn, ACS Nano **15**, 5449 (2021).
[16] M. M. Ugeda, D. Fernández-Torre, I. Brihuega, P. Pou, A. J. Martínez-Galera, R. Pérez, and J. M. Gomez-Rodriguez, Point defects on graphene on metals, Phys. Rev. Lett. **107**, 116803 (2011).
[17] F. Long, M. Ghorbani-Asl, K. Mosina, Y. Li, K. Lin, F. Ganss, R. Hübner, Z. Sofer, F. Dirnberger, A. Kamra, A. V. Krasheninnikov, S. Prucnal, M. Helm, and S. Zhou, Ferromagnetic interlayer coupling in CrSBr crystals irradiated by ions, Nano Lett. **23**, 8468 (2023).
[18] X. Gao, B. Jiang, A. E. L. Allcca, K. Shen, M. A. Sadi, A. B. Solanki, P. Ju, Z. Xu, P. Upadhyaya, Y. P. Chen, S. A. Bhave, and T. Li, High-contrast plasmonic-enhanced shallow spin defects in hexagonal boron nitride for quantum sensing, Nano Lett. **21**, 7708 (2021).
[19] U. Bangert, W. Pierce, D. M. Kepaptsoglou, Q. Ramasse, R. Zan, M. H. Gass, J. A. den Berg, C. B. Boothroyd, J. Amani, and H. Hofsäss, Ion implantation of graphene–toward IC compatible technologies, Nano Lett. **13**, 4902 (2013).
[20] U. Bangert, A. Stewart, E. O'Connell, E. Courtney, Q. Ramasse, D. Kepaptsoglou, H. Hofsäss, J. Amani, J. S. Tu, and B. Kardynal, Ion-beam modification of 2-D materials - single implant atom analysis via annular dark-field electron microscopy, Ultramicroscopy **176**, 31 (2017).
[21] T. Susi, T. P. Hardcastle, H. Hofsäss, A. Mittelberger, T. J. Pennycook, C. Mangler, R. Drummond-Brydson, A. J. Scott, J. C. Meyer, and J. Kotakoski, Single-atom spectroscopy of phosphorus dopants implanted into graphene, 2D Mater. **4**, 021013 (2017).
[22] M. Tripathi, A. Markevich, R. Böttger, S. Facsko, E. Besley, J. Kotakoski, and T. Susi, Implanting germanium into graphene, ACS Nano **12**, 4641 (2018).
[23] M. N. Bui, S. Rost, M. Auge, J.-S. Tu, L. Zhou, I. Aguilera, S. Blügel, M. Ghorbani-Asl, A. V. Krasheninnikov, A. Hashemi, H.-P. Komsa, L. Jin, L. Kibkalo, E. N. O'Connell, Q. M. Ramasse, U. Bangert, H. C. Hofsäss, D. Grützmacher, and B. E. Kardynal, Low-energy se ion implantation in $MoS_2$ monolayers, npj 2D Mater. Appl. **6**, 42 (2022).
[24] R. Villarreal, Z. Zarkua, S. Kretschmer, V. Hendriks, J. Hillen, H. C. Tsai, F. Junge, M. Nissen, T. Saha, S. Achilli, H. C. Hofsäss, M. Martins, G. De Ninno, P. Lacovig, S. Lizzit, G. Di Santo, L. Petaccia, S. De Feyter, S. De Gendt, S. Brems *et al.*, Achieving high substitutional incorporation in Mn-doped graphene, ACS Nano **18**, 17815 (2024).
[25] P. Willke, J. A. Amani, A. Sinterhauf, S. Thakur, T. Kotzott, T. Druga, S. Weikert, K. Maiti, H. Hofsäss, and M. Wenderoth,

Doping of graphene by low-energy ion meam implantation: Structural, electronic, and transport properties, Nano Lett. **15**, 5110 (2015).

[26] M. Telychko, K. Noori, H. Biswas, D. Dulal, P. Lyu, J. Li, H.-Z. Tsai, H. Fang, Z. Qiu, Z. W. Yap, K. Watanabe, T. Taniguchi, M. F. Crommie, A. Rodin, and J. Lu, Gate-tunable artificial nucleus in graphene, arXiv:2111.09149.

[27] H. Wang, Q. Wang, Y. Cheng, K. Li, Y. Yao, Q. Zhang, C. Dong, P. Wang, U. Schwingenschlögl, W. Yang, and X. X. Zhang, Doping monolayer graphene with single atom substitutions, Nano Lett. **12**, 141 (2012).

[28] Q. Ma, M. Isarraraz, C. S. Wang, E. Preciado, V. Klee, S. Bobek, K. Yamaguchi, E. Li, P. M. Odenthal, A. Nguyen, D. Barroso, D. Sun, G. Von Son Palacio, M. Gomez, A. Nguyen, D. Le, G. Pawin, J. Mann, T. F. Heinz, T. S. Rahman *et al.*, Postgrowth tuning of the bandgap of single-layer molybdenum disulfide films by sulfur/selenium exchange, ACS Nano **8**, 4672 (2014).

[29] Q. Ma, P. M. Odenthal, J. Mann, D. Le, C. S. Wang, Y. Zhu, T. Chen, D. Sun, K. Yamaguchi, T. Tran, M. Wurch, J. L. McKinley, J. Wyrick, K. Magnone, T. F. Heinz, T. S. Rahman, R. Kawakami, and L. Bartels, Controlled argon beam-induced desulfurization of monolayer molybdenum disulfide, J. Phys.: Condens. Matter **25**, 252201 (2013).

[30] Program TRIM (2008) by J.F. Ziegler and J.P. Biersack, http://www.srim.org.

[31] W. Möller, W. Eckstein, and J. Biersack, Tridyn-binary collision simulation of atomic collisions and dynamic composition changes in solids, Comput. Phys. Commun. **51**, 355 (1988).

[32] K. Nordlund and F. Djurabekova, Multiscale modelling of irradiation in nanostructures, J. Comput. Electron. **13**, 122 (2014).

[33] E. H. Ahlgren, J. Kotakoski, O. Lehtinen, and A. V. Krasheninnikov, Ion irradiation tolerance of graphene as studied by atomistic simulations, Appl. Phys. Lett. **100**, 233108 (2012).

[34] S. Zhao and J. Xue, Tuning the band gap of bilayer graphene by ion implantation: Insight from computational studies, Phys. Rev. B **86**, 165428 (2012).

[35] S. Kretschmer, S. Ghaderzadeh, S. Facsko, and A. V. Krasheninnikov, Threshold ion energies for creating defects in 2d materials from first-principles calculations: Chemical interactions are important, J. Phys. Chem. Lett. **13**, 514 (2022).

[36] G. Kresse and J. Hafner, *Ab initio* molecular dynamics for liquid metals, Phys. Rev. B **47**, 558 (1993).

[37] G. Kresse and J. Furthmüller, Efficiency of *ab-initio* total energy calculations for metals and semiconductors using a plane-wave basis set, Comput. Mater. Sci. **6**, 15 (1996).

[38] J. P. Perdew, K. Burke, and M. Ernzerhof, Generalized gradient approximation made simple, Phys. Rev. Lett. **77**, 3865 (1996).

[39] M. Caro, A. A. Correa, E. Artacho, and A. Caro, Stopping power beyond the adiabatic approximation, Sci. Rep. **7**, 2618 (2017).

[40] A. Niggas, L. Fischer, S. Kretschmer, M. Werl, H. Biber, C. Speckmann, N. McEvoy, J. Kotakoski, F. Aumayr, A. V. Krasheninnikov, and R. A. Wilhelm, Charge-exchange-dependent energy loss of H and He in freestanding monolayers of graphene and $MoS_2$, Phys. Rev. A **108**, 062823 (2023).

[41] A. Schleife, Y. Kanai, and A. A. Correa, Accurate atomistic first-principles calculations of electronic stopping, Phys. Rev. B **91**, 014306 (2015).

[42] M. A. Zeb, J. Kohanoff, D. Sánchez-Portal, A. Arnau, J. I. Juaristi, and E. Artacho, Electronic stopping power in gold: The role of d electrons and the H/He anomaly, Phys. Rev. Lett. **108**, 225504 (2012).

[43] A. P. Thompson, H. M. Aktulga, R. Berger, D. S. Bolintineanu, W. M. Brown, P. S. Crozier, P. J. in 't Veld, A. Kohlmeyer, S. G. Moore, T. D. Nguyen, R. Shan, M. J. Stevens, J. Tranchida, C. Trott, and S. J. Plimpton, LAMMPS - a flexible simulation tool for particle-based materials modeling at the atomic, meso, and continuum scales, Comput. Phys. Commun. **271**, 108171 (2022).

[44] J. F. Ziegler and J. P. Biersack, The stopping and range of ions in matter, in *Treatise on Heavy-Ion Science: Astrophysics, Chemistry, and Condensed Matter*, edited by D. A. Bromley (Boston, MA, 1985), Vol. 6, pp. 93–129.

[45] J. F. Ziegler, J. P. Biersack, and U. Littmark, *The Stopping and Range of Ions in Solids* (Pergamon, New York, 1985).

[46] A. Kınacı, J. B. Haskins, C. Sevik, and T. Çağin, Thermal conductivity of BN-C nanostructures, Phys. Rev. B **86**, 115410 (2012).

[47] E. H. Ahlgren, J. Kotakoski, and A. V. Krasheninnikov, Atomistic simulations of the implantation of low-energy boron and nitrogen ions into graphene, Phys. Rev. B **83**, 115424 (2011).

[48] T. Susi, C. Hofer, G. Argentero, G. T. Leuthner, T. J. Pennycook, C. Mangler, J. C. Meyer, and J. Kotakoski, Isotope analysis in the transmission electron microscope, Nat. Commun. **7**, 13040 (2016).

[49] M. Kalbac, O. Lehtinen, A. V. Krasheninnikov, and J. Keinonen, Ion-irradiation-induced defects in isotopically-labeled two layered graphene: Enhanced *in-situ* annealing of the damage, Adv. Mater. **25**, 1004 (2013).

[50] S. Kretschmer, M. Maslov, S. Ghaderzadeh, M. Ghorbani-Asl, G. Hlawacek, and A. V. Krasheninnikov, Supported two-dimensional materials under ion irradiation: The substrate governs defect production, ACS Appl. Mater. Interfaces **10**, 30827 (2018).

[51] J. P. Thiruraman, P. Masih Das, and M. Drndić, Irradiation of transition metal dichalcogenides using a focused ion beam: Controlled single-atom defect creation, Adv. Funct. Mater. **29**, 1904668 (2019).

[52] E. van der Giessen, P. A. Schultz, N. Bertin, V. V. Bulatov, W. Cai, G. Csányi, S. M. Foiles, M. G. D. Geers, C. González, M. Hütter, W. K. Kim, D. M. Kochmann, J. LLorca, A. E. Mattsson, J. Rottler, A. Shluger, R. B. Sills, I. Steinbach, A. Strachan, and E. B. Tadmor, Roadmap on multiscale materials modeling, Modell. Simul. Mater. Sci. Eng. **28**, 043001 (2020).

[53] N. Fedik, R. Zubatyuk, M. Kulichenko, N. Lubbers, J. S. Smith, B. Nebgen, R. Messerly, Y. W. Li, A. I. Boldyrev, K. Barros, O. Isayev, and S. Tretiak, Extending machine learning beyond interatomic potentials for predicting molecular properties, Nat. Rev. Chem. **6**, 653 (2022).

[54] www.gauss-centre.eu.

[55] www.hlrs.de.